Underwater vehicle guidance control design within the DexROV project: preliminary results ⋆

Daniela De Palma and **Giovanni Indiveri**

Dipartimento Ingegneria Innovazione, University of Salento - ISME Node - 73100, Lecce, Italy (e-mail: name.lastname@unisalento.it).

Abstract: The paper addresses the guidance (i.e. kinematics based) control design of the motion controller for an underwater remotely operated vehicle (ROV) within an European Commission H2020 research project called DexROV. Given a kinematics model of an ROV eventually subject to an ocean current, the problem consists in designing a guidance control law able to realize, within a common and unified framework, several basic control loops denoted as "primitives". The problem is rather standard when considering such primitives individually, but it becomes more challenging when aiming at designing a single general solution able to realize several different primitives according on how the reference signal for the controller is assigned. Moreover, the proposed guidance loop is required to operate in the presence of possible delays with the base station. The proposed solution builds on standard techniques leading to a proportional - integral (PI) controller with an adaptive gain selection rule to cope with possible integrator wind-up phenomena due to vehicle velocity saturation. The designed solution is numerically tested and analysed through simulations accounting for simplified, yet realistic, sensor models including stochastic noise and delays.

Keywords: marine systems, ROV, guidance, communication latencies.

1. INTRODUCTION

DexROV: Dexterous Undersea Inspection and Maintenance in Presence of Communication Latencies is an ongoing european research projects funded by the European Commission (EC) under the H2020 Research and Innovation programme. DexROV aims at the development of new underwater service capabilities with a focus on far distance teleoperation of Remotely Operated Vehicles (ROVs) involving variable communication latencies. In particular, the ROV pilot console within the DexROV project will be in a separate physical location (Onshore Control Center, OCC) with respect to the surface end of the ROV tether where guidance commands will be elaborated (Offshore Operations). The OCC will communicate with the ROV system through a satellite link exhibiting possibly non negligible delays. Moreover, the project vehicle will be equipped with a pair of manipulators. Indeed a second focus of the project is on advanced dexterous manipulation capabilities benefiting from context specific human skills and know-how also over long distances Gancet et al. (2015). The project is 3.5 years long and has started in March 2015.

This paper addresses the design of the guidance control system for the DexROV vehicle to be integrated with its navigation and actuator control systems as well as with the manipulator controller. Indeed the higher level specifications for the ROV guidance system are rather standard, yet the requirements related to a near-future integration with a specific manipulator control system and an ad-hoc navigation system suggest to aim at designing a *generic* guidance solution able to implement, within the very same kinematics control law, several different basic motion control loops. These will be called DexROV vehicle *primitives* in the following and include:

(1) Hovering (dynamic positioning)
(2) Autodepth
(3) Autoheading
(4) Autoaltitude
(5) Guidance from point A to point B.

The original contribution of the paper is related to the design of a single kinematics control solution able to seemingly implement all the requested primitives within a unique and general framework. Notice that from a technological point of view, the basic motion control functionalities associated with the listed primitives are rather standard as accounted for, by example, in Christ and Wernli (2014) and Fossen (2011). Indeed, starting from the pioneering work of Yoerger et al. (1986), many advanced motion control solutions for ROVs have been designed and tested in the last 30 years. Although the performance of such solutions will depend on the available specific actuation system (lower level control layer) and navigation system, at a guidance level (kinematics control layer) the motion control primitives can be designed independently of these sub-systems. Indeed, the preliminary results described in this paper refer to a solution based on a purely

⋆ This work was partially supported by EC Horizon 2020 programme under the project DexROV (Grant number: 635491). DexROV contributes to the "Blue Growth" long term European strategy to support sustainable growth in the marine and maritime sectors.

kinematics model of the ROV. As a result, the controller is a proportional - integral (PI) closed loop law. For the sake of brevity, the DexROV navigation system will not be described in detail. As illustrated in the following, only some basic assumptions on the available feedback will be made and their impact on the proposed guidance laws will be discussed. Essentially, the necessary feedback needed to close the loop is related to the position and velocity estimated of the vehicle as usually needed in dynamic positioning (DP) applications Sørensen (2011), Sørensen et al. (2012), Sørensen (2014). The proposed kinematics solution is numerically simulated including a simplified, yet realistic, model of ultra short base line (USBL) positioning system having a relatively low sampling frequency and a delay that is range dependent. Indeed, given such range dependent delay, the described simulation analysis suggests that the very kinematics control can benefit from using adaptive gains as also discussed in the literature (Hoang and Kreuzer (2007)) for dynamic model based controllers of ROVs.

After describing the adopted notation and the guidance design methodology in sections 2 and 3 the motion primitive results are illustrated in section 4. Finally numerical results and conclusions are addressed in sections 5 and 6 respectively.

2. NOTATION

The notation adopted in this paper is rather standard. For the sake of clarity and completeness we report the most significant notation details.

Vectors will be denoted in bold face fonts while matrices will be denoted by capital regular (not bold) fonts. Rotation matrices (i.e. elements of the special orthogonal group $SO(n)$ with n being 3 unless otherwise stated) will be indicated as ${}^1R_0$ being 0 and 1 the labels of the input and output frames respectively. Namely indicating with ${}^0\mathbf{b}$ the projection of vector $\mathbf{b}$ in frame 0, its components in frame 1 will be given by ${}^1\mathbf{b} = {}^1R_0\,{}^0\mathbf{b}$. Indeed, denoting with $\mathbf{i}_0, \mathbf{j}_0$ and $\mathbf{k}_0$ the unit vectors of frame 0, the rotation matrix ${}^1R_0$ results in

$$ {}^1R_0 = \begin{bmatrix} {}^1\mathbf{i}_0 & {}^1\mathbf{j}_0 & {}^1\mathbf{k}_0 \end{bmatrix} $$

where ${}^1\mathbf{i}_0$, ${}^1\mathbf{j}_0$ and ${}^1\mathbf{k}_0$ are the projections of $\mathbf{i}_0, \mathbf{j}_0$ and $\mathbf{k}_0$ in frame 1.

The cross product $\mathbf{a} = \mathbf{b} \times \mathbf{c}$ among elements in $\mathbb{R}^3$ expressed as components with respect to a given frame can be computed as a matrix times vector operation in the form

$$ \mathbf{a} = \mathbf{b} \times \mathbf{c} = S(\mathbf{b})\,\mathbf{c} $$

being the skew symmetric matrix $S(\cdot)$ given by

$$ S(\mathbf{b}) = \begin{pmatrix} 0 & -b_3 & b_2 \\ b_3 & 0 & -b_1 \\ -b_2 & b_1 & 0 \end{pmatrix}. \tag{1} $$

3. KINEMATIC GUIDANCE DESIGN

3.1 Modelling and linear velocity control

$$ \dot{\mathbf{p}} = \mathbf{u} + \mathbf{v}_c \tag{2} $$

$$ {}^1\dot{R}_0 = -S({}^1\boldsymbol{\omega}_{1/0})\,{}^1R_0. \tag{3} $$

The control input is the velocity with respect to the fluid $\mathbf{u} \in \mathbb{R}^3$, namely the linear motion model is fully actuated and eventually subject to a (matched) disturbance $\mathbf{v}_c$ representing the ocean current. The rotation matrix ${}^1R_0$ maps vectors from frame 0 to frame 1: in particular frame 0 is assumed to be an earth fixed frame (typically a North East Down - NED frame) and frame 1 is a body fixed frame having its x, y, z axis aligned to surge, sway and heave directions of the ROV. In the following, unless otherwise stated, equation (2) will be thought as expressed in frame 1: namely $\dot{\mathbf{p}}$ is the ROV velocity as projected in body frame. Assuming the desired position to be $\mathbf{p}_d$ having velocity $\dot{\mathbf{p}}_d$, the position error would be

$$ \mathbf{e} = \mathbf{p}_d - \mathbf{p}. \tag{4} $$

Its time evolution (in body frame) is

$$ \dot{\mathbf{e}} = \dot{\mathbf{p}}_d - \mathbf{u} - \mathbf{v}_c \tag{5} $$

suggesting for the control input $\mathbf{u}$ a PI with feedforward structure

$$ \mathbf{u} = K_p\,\mathbf{e} + K_I \int_{t_i}^{t} \mathbf{e}(\tau)d\tau + \hat{\dot{\mathbf{p}}}_d - \hat{\mathbf{v}}_c \tag{6} $$

where $\hat{\dot{\mathbf{p}}}_d$ and $\hat{\mathbf{v}}_c$ are estimates (to be defined) of the desired velocity and ocean current. Assume

$$ \hat{\dot{\mathbf{p}}}_d - \dot{\mathbf{p}}_d = \boldsymbol{\delta}_1 \quad : \quad \dot{\boldsymbol{\delta}}_1 = \mathbf{0} \tag{7} $$

$$ \hat{\mathbf{v}}_c - \mathbf{v}_c = \boldsymbol{\delta}_2 \quad : \quad \dot{\boldsymbol{\delta}}_1 = \mathbf{0} \tag{8} $$

that can be satisfied, by example, if $\dot{\mathbf{p}}_d$ and $\mathbf{v}_c$ are constant and their estimates are null. If assumption (7 - 8) hold, the closed loop error would evolve as

$$ \dot{\mathbf{e}} = \dot{\mathbf{p}}_d - \mathbf{v}_c - K_p\,\mathbf{e} - K_I \int_{t_i}^{t} \mathbf{e}(\tau)d\tau - \hat{\dot{\mathbf{p}}}_d + \hat{\mathbf{v}}_c = \tag{9} $$

$$ = -K_p\,\mathbf{e} - K_I \int_{t_i}^{t} \mathbf{e}(\tau)d\tau - \boldsymbol{\delta}_1 + \boldsymbol{\delta}_2 \tag{10} $$

namely

$$ \ddot{\mathbf{e}} + K_p\dot{\mathbf{e}} + K_I\mathbf{e} = \mathbf{0} \tag{11} $$

implying an exponential convergence of $\mathbf{e}$ to zero if K_p and K_I are positive definite matrices.

Notice that constant ocean currents in the earth fixed frame

$$ \frac{d}{dt}\,{}^0\mathbf{v}_c = \mathbf{0} $$

will generally be time varying in body frame. Likewise, if the desired position should be moving at constant velocity in an earth fixed frame, it will generally be time varying in body frame. Nevertheless, for sufficiently smooth motions of the ROV (i.e. with sufficiently small curvature and torsion) and for sufficiently small values (in earth frame) of $\dot{\mathbf{p}}_d$ and $\mathbf{v}_c$, the above hypothesis (7 - 8) are reasonable and will be, at least approximately, satisfied. With reference to (11), the gain matrices K_p and K_I can be chosen such to force a decoupled second order dynamics on the error components. In particular, making use of the standard notation for second order systems, i.e. denoting with ξ the damping coefficient and ω_n the natural frequency, the K_p and K_I matrices are suggested to be

$$ K_p = 2\,\mathrm{diag}(\xi_1\omega_{n1},\ \xi_2\omega_{n2},\ \xi_3\omega_{n3}) \tag{12} $$

$$ K_I = \mathrm{diag}(\gamma_1\,\omega_{n1}^2,\ \gamma_2\,\omega_{n2}^2,\ \gamma_3\,\omega_{n3}^2) \tag{13} $$

with

$$\xi_h \in \left[\frac{\sqrt{2}}{2}, 1\right] \quad \forall \;\; h = 1, 2, 3$$

to have a sufficiently large phase margin. Also ξ should not exceed 1 to prevent one the two poles going towards the origin (indeed the slow pole of a second order system tends to $-\omega_n/(2\xi)$ when $\xi >> 1$). The γ_h values are parameters set to 1 or 0 for anti wind-up purposes as described below.

Recalling that $\mathbf{u} = (u, v, w)^\top$ is a body reference velocity command in surge (u), sway (v) and heave (w) and considering the maximum surge $u_{\max} > 0$, sway $v_{\max} > 0$ and heave $w_{\max} > 0$ velocities of the ROV, the proportional gains (12) can be heuristically fixed as follows:

$$\omega_{n1} = \frac{u_{\max}}{2\xi_1 \; \bar{e}_u} \tag{14}$$

$$\omega_{n2} = \frac{v_{\max}}{2\xi_2 \; \bar{e}_v} \tag{15}$$

$$\omega_{n3} = \frac{w_{\max}}{2\xi_3 \; \bar{e}_w} \tag{16}$$

being $\bar{e}_u, \bar{e}_v$ and $\bar{e}_w$ the threshold values of distances to the target along surge, sway and heave when to go at maximum speed (i.e. when to saturate the ROV velocity).

In order to deal with wind-up issues related to the integral action of the proposed controller, the integral gain K_I should be set to zero if the error components exceed the saturation threshold. Hence the γ_h values in (13) will be selected as

$$\gamma_1 = \begin{cases} 1 \text{ if } |e_u| \leq \bar{e}_u \\ 0 \text{ otherwise} \end{cases} \tag{17}$$

$$\gamma_2 = \begin{cases} 1 \text{ if } |e_v| \leq \bar{e}_v \\ 0 \text{ otherwise} \end{cases} \tag{18}$$

$$\gamma_3 = \begin{cases} 1 \text{ if } |e_w| \leq \bar{e}_w \\ 0 \text{ otherwise} \end{cases} \tag{19}$$

For the digital implementation of the continuous PI controller its transfer function can be discretized using Tustin's (bilinear) method consisting in mapping the continuos time laplace variable s in the discrete time z variable as

$$s \;\longmapsto\; 2\,\frac{z-1}{(z+1)\,\delta_T} \tag{20}$$

being δ_T the sampling time. This leads to the following discrete time version of the control law (6):

$$K_1 := K_p + \frac{K_I\,\delta_T}{2} \tag{21}$$

$$K_2 := \frac{K_I\,\delta_T}{2} - K_p \tag{22}$$

$$\mathbf{u}(k+1) = \mathbf{u}(k) + K_1\,\mathbf{e}(k+1) + K_2\,\mathbf{e}(k) + \hat{\dot{\mathbf{p}}}_d - \hat{\mathbf{v}}_c \tag{23}$$

where $\mathbf{u}$ is the linear velocity command in body frame.

3.2 Heading control

Although the ROV has fully actuated linear velocities, i.e. it can *crab*, control authority over surge is higher than on the sway axis. Moreover, cameras and obstacle avoidance sonars are often forward looking (i.e. in surge direction), so for longer distance movements the preferred traveling direction should indeed be surge. In order to accomplish this objective, assuming that the ROV has null or negligible pitch and roll angles, the position error vector $\mathbf{e}$ in body frame should preferably be oriented along the vehicle's surge axis. The required heading can hence be computed as follows

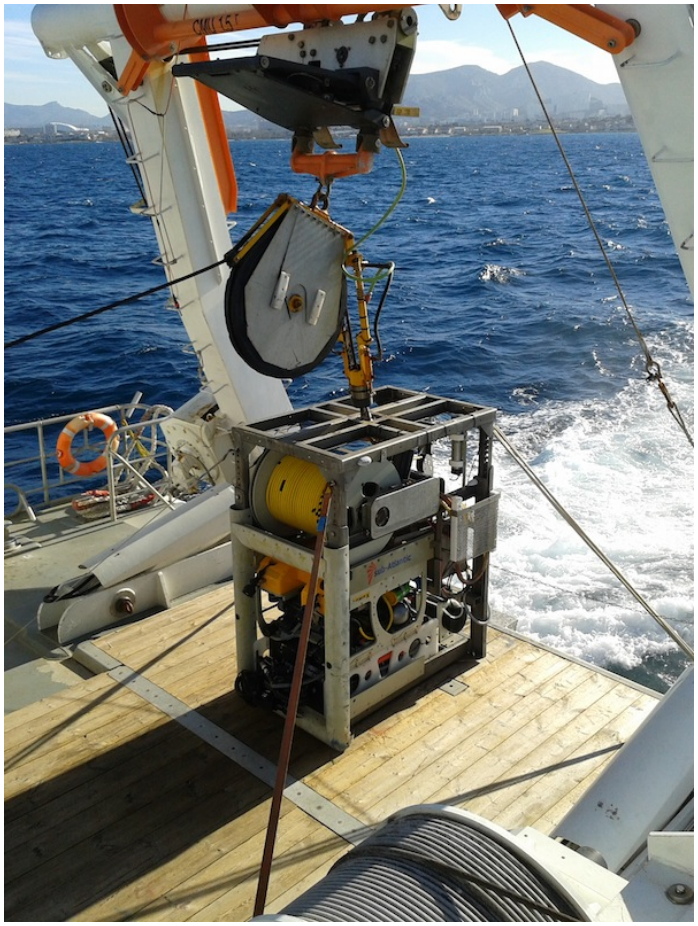

Fig. 1. DexROV ROV

$$\psi_{surge} = \text{atan2}\left(\frac{e_2}{\sqrt{e_1^2 + e_2^2}}, \frac{e_1}{\sqrt{e_1^2 + e_2^2}}\right) \tag{24}$$

being $\mathbf{e} = (e_1, e_2, e_3)^\top$ the position error in body frame assuming the horizontal plane error $\sqrt{e_1^2 + e_2^2} > \varepsilon$. The value of the ε threshold needs to be chosen as a function of the accuracy used to measure $\mathbf{e}$ in order to avoid discontinuities in the computed values of ψ_{surge} given by (24) for vanishing values of $\mathbf{e}$. Of course, the heading reference may also be assigned independently: in general the yaw reference will be denoted as ψ_d such that the heading error variable $\tilde{\psi}$ can either be $\psi_d - \psi$ or ψ_{surge} in (24). In the latter case, the control will be referred to as *auto surge heading*. A pictorial representation of the ψ_{surge} reference for auto surge heading control is reported in figure (2).

The yaw controller is also designed as a PI velocity controller, namely given the kinematic model

$$\dot{\psi} = r \tag{25}$$

having the yaw rate r as input, the yaw error dynamics is given by

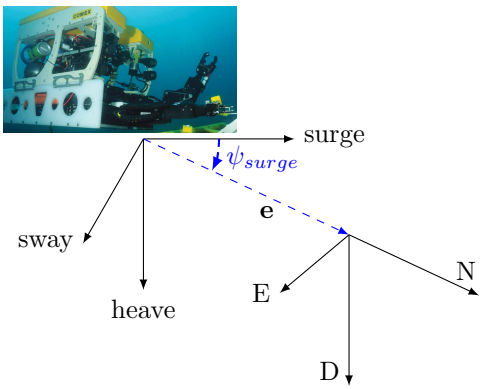

Fig. 2. Frame kinematics

$$\tilde{\psi} := \psi_d - \psi \tag{26}$$

$$\dot{\tilde{\psi}} = \dot{\psi}_d - r \tag{27}$$

suggesting a controller as

$$r = k_{p\psi}\,\tilde{\psi} + k_{I\psi}\int_{t^*}^{t}\tilde{\psi}(\tau)d\tau + \hat{\dot{\psi}}_d \tag{28}$$

where the proportional and integral gains will be computed following the same line of thought illustrated for the linear velocity case. Namely

$$k_{p\psi} = 2\,\xi_\psi\,\omega_{n\psi} \tag{29}$$

$$k_{I\psi} = \gamma_r\,\omega_{n\psi}^2 \tag{30}$$

$$\xi_\psi \in \left[\sqrt{2}/2,\ 1\right] \tag{31}$$

$$\omega_{n\psi} = \frac{r_{\max}}{2\,\xi_\psi\,\bar{\bar{\psi}}} \tag{32}$$

being $\bar{\bar{\psi}} > 0$ the size of the heading error for which maximum yaw rate should be commanded. To cope with wind-up issues, the integral action on yaw rate command is excluded when the yaw error exceeds $\bar{\bar{\psi}}$, namely γ_r is computed as

$$\gamma_r = \begin{cases} 1 \text{ if } |\tilde{\psi}| \le \bar{\bar{\psi}} \\ 0 \text{ otherwise} \end{cases}. \tag{33}$$

Notice that if $\tilde{\psi}$ should be defined as ψ_{surge} in (24) it would belong to the set $[-180, 180]$ (in degrees). Likewise, should ψ_d be defined by the user or by other means, it would be anyhow forced to belong to the same set $[-180, 180]$. It follows that depending on the yaw angle $\psi \in [-180, 180]$ of the vehicle, the yaw orientation error $\tilde{\psi}$ in (26) could be such that $|\tilde{\psi}| > 180$ resulting in a turn going the opposite direction with respect to the closest yaw direction aligning the vehicle with the desired orientation. To prevent this behavior, in implementing the proposed controller, the yaw error $\tilde{\psi}$ is *wrapped* as follows

$$\text{if } \left|\tilde{\psi}\right| > 180 \implies \tilde{\psi} \longmapsto \tilde{\psi} - 360\,\text{sign}\left(\tilde{\psi}\right) \tag{34}$$

being $\text{sign}(\cdot)$ the sign function sign: $\mathbb{R} \longrightarrow \{-1, 0, 1\}$ defined as

$$\text{sign}(\alpha) = \begin{cases} +1 & \text{if } \alpha > 0 \\ 0 & \text{if } \alpha = 0 \\ -1 & \text{if } \alpha < 0 \end{cases} \tag{35}$$

for any real number α. Following the discussion outlined for the linear velocity case, the discrete time version of the PI control law for yaw rate results in

$$K_3 := k_{p\psi} + \frac{k_{I\psi}\,\delta_T}{2} \tag{36}$$

$$K_4 := \frac{k_{I\psi}\,\delta_T}{2} - k_{p\psi} \tag{37}$$

$$r(k+1) = r(k) + K_3\,\tilde{\psi}(k+1) + K_4\,\tilde{\psi}(k) + \hat{\dot{\psi}}_d. \tag{38}$$

4. MOTION PRIMITIVES

As described in the section 1, the desired DexROV motion primitives shall consist in the following:

(1) Hovering (dynamic positioning)
(2) Autodepth
(3) Autoheading
(4) Autoaltitude
(5) Guidance from point A to point B,

Interestingly all such primitives (and others that can be defined by superposition) can be achieved through the very same control laws (23) and (38) by suitably defying the reference values $\mathbf{p}_d$ and ψ_d. In particular, the above motion primitives can all be thought as variants of the *guidance from point A to point B*. In principle the motion control problem of going from A to B can be solved with a linear velocity given through (6, 23) and an arbitrary heading. Yet, as previously discussed, the surge direction may be preferable given the enhanced control authority in such direction as well as the presence of specific sensors mounted in the surge direction. This is why the heading reference to be followed thanks to the control law (28, 38) is either an arbitrary ψ_d or the one pointing to the target point B. Of course, if the heading control with reference ψ_d is implemented without activating any linear velocity, this would correspond to an Autoheading primitive. Likewise, if the target point B should be located on the vertical passing through the origin of the ROV body frame, this would correspond to an Autodepth (or Autoaltitude) primitive.

Data: $\mathbf{p}_d$ and ψ_d
Result: Yaw velocity motion control primitives
initialization;
read ψ_d;
if *ψ_d is defined in SW interface (not void)* **then**
  set $\tilde{\psi} = \psi_d - \psi$;
else
  if *$(p_d)_x$ & $(p_d)_y$ are defined* **then**
    set $\tilde{\psi} = \psi_{surge}$ according to (24);
  else
    set $\tilde{\psi}$ = void;
  end
end
if *$\tilde{\psi}$ not void & larger than threshold* **then**
  execute (38);
else
  $r = 0$;
end

Algorithm 1: Yaw controller

It hence follows that the necessary DexROV motion control primitives can be all implemented by the control laws (23) and (38) with suitably defined references and error variables. In particular the software interface to launch the control laws (23) and (38) will allow to define (def) or not (void) the individual components of the desired position vector $\mathbf{p}_d = ((p_d)_x, (p_d)_y, (p_d)_z)^\top$ and heading ψ_d. The logic being that if a reference component is not defined (i.e. it is void), the corresponding error component in the control laws (23) and (38) will be set to zero. More specifically, the logic will be as outlined in Algorithms (1) and (2):

Data: $\mathbf{p}_d$ and $\mathbf{p}$
Result: Linear velocity motion control primitives initialization;
read $\mathbf{p}_d$ and $\mathbf{p}$;
for $h = \{x, y, z\}$ **do**
  if $(p_d)_h$ *is void* **then**
    set $(u)_h = 0$;
  else
    $(e)_h = (p_d)_h - (p)_h$;
    if $(e)_h$ *greater than threshold* **then**
      execute h component of (23)
    end
  end
end

Algorithm 2: Surge controller ($\mathbf{p}$ and $\mathbf{p}_d$ are in body frame).

5. SIMULATOR STRUCTURE AND PRELIMINARY RESULTS

The proposed guidance control laws have been validated numerically using a simplified, yet realistic, simulator of the scenario under investigation. The simulator has been developed in Matlab. It includes the following major modules: i) the purely kinematic model of the ROV (2-3), ii) the guidance control system, iii) the sensors feedbacks iv) the communication module including delay and v) the graphics display. Regarding the kinematic model, a minimal disturbance on the roll and pitch rates has been added to equation (3) aiming at making a more realistic simulation of the ROV attitude. A saturation of the velocity commands to the maximum surge, sway and heave velocities has also been implemented. As discussed in section 3, the ocean current $\mathbf{v}_c$ is assumed to be constant in NED frame and slowly varying in body frame: consequently its effect will be almost completely rejected by the integral action of the controller. In light of the robustness granted by the integral action of the controller, and for the sake of simplicity, an observer for the ocean current velocity $\mathbf{v}_c$ is not included in this work. In particular, the term $\hat{\mathbf{v}}_c$ in (6) is omitted. With reference to the guidance system, the control loop is closed using the measurements from USBL (for x and y coordinates in NED frame), depth sensor (for z coordinate in NED frame) and AHRS (for roll, pitch and yaw angles, i.e. ϕ, θ, ψ). A sampling frequency of 10 Hz has been assumed for measurements from depth sensor and AHRS. The measurement uncertainty has been modelled as gaussian noise with standard deviation equal to 2 [m] and 1 [deg] for the depth sensor and AHRS, respectively, in accordance with the specifications of the currently available DexROV devices. A simplified and realistic model of USBL positioning system have been simulated having a relatively low sampling frequency (approximately 1 Hz) and a delay that is range dependent (namely two times the range divided by the velocity of the sound in water). The measurement accuracy is also range dependent: for the DexROV USBL, and in compliance with the system data sheets, it is 1% of the slant range.

$(p_d)_x$	$(p_d)_y$	$(p_d)_z$	ψ_d	Primitive
def	def	def / void	void	A to B with auto surge heading
def	def	def	def	A to B with no autosurge heading (includes hovering)
void	def	def / void	def / void	sway correction and no auto-surge heading
def	void	def / void	def / void	surge correction and no auto-surge heading
void	void	def	void	autodepth / altitude
void	void	void	def	autoheading

Table 1. Primitive examples depending on the target references.

The simulator simultaneously displays in two views (left-view and right-view in figure 3): i) the Onshore Control Center (OCC) user interface including the ROV position as it is available to OCC through the telemetry acquired by the (possibly delayed) satellite communication link and ii) the Offshore Operations: the instructions received from the OCC operator with satellite communication delay and the actual ROV position and orientation. The inputs to the simulator are the individual components of the desired position and heading of the ROV. Based on the definition or not of the desired components, the proposed guidance control law implements the proper motion primitives. The described simulator has been used to undertake a preliminary validation of the controller performance for the DexROV motion primitives. In particular, two scenarios at different depth (10 and 1000 $[m]$) are presented in the following. The initial position of the ROV is fixed at $(10, 10, 10)[m]$ in the earth fixed frame. The USBL is assumed to be located at the origin of the earth fixed frame and a constant ocean current in the horizontal plane has been simulated, i.e. ${}^0\mathbf{v}_c = (0.1, 0.1, 0)[m/s]$. In both scenarios only the x and y components of the desired positions (i.e. (80, 80)$[m]$) are specified, the z component and heading are kept void. This leads to the activation of two primitives simultaneously: (2) Autodepth and (5) Guidance from point A to point B with *auto surge heading*. The parameters used for the definition of the controllers gains are reported in table 2.

Surge Controller	Yaw Controller
$\xi_{1,2,3} = 1$	$\xi_\psi = 1$
$u_{max} = 1\,[m/s]$ $v_{max} = 0.5\,[m/s]$ $w_{max} = 0.5\,[m/s]$	$r_{max} = 120\,[deg/s]$
$\bar{e}_u = 5\,[m]$ $\bar{e}_v = 5\,[m]$ $\bar{e}_w = 5\,[m]$	$\bar{\tilde{\psi}} = 120\,[deg]$

Table 2. Parameters for controllers gains.

The figures 4, 5 and 6 report the trajectory and the linear and angular velocity commands, respectively, related to the first simulation scenario at low depth (10 $[m]$). The controller gains are tuned as described in section 3 using the parameters reported in table 2. As expected, the proposed control solution is able to activate and execute the necessary motion primitives. Indeed, the target position is correctly reached with a travelling direction oriented along the vehicle's surge axis. At the same time, the depth is kept approximately constant to the initial value in accordance with the Autodepth primitive. The figures 7, 8 and 9 report the trajectory and the linear and angular velocity commands, respectively, related to the second simulation scenario at higher depth (1000 $[m]$). In this scenario two different controllers gains have been compared. In the above mentioned figures, the results related to the higher gain are depicted in blue, whereas those ones related to the lower gain are depicted in red. It is worth highlighted that the higher gain is actually the same used in the first low depth scenario. The corresponding trajectory appears to be nonlinear (blue line in figure 7). This phenomena is due to the fact that the increase of the depth leads to both: an increase of the delay in the USBL measurements acquisition and an increase of the USBL measurement errors; as noticed previously, they are both function of the range. This phenomena can be mitigated reducing the gains of the controllers. Indeed, reducing the natural frequency coefficients (14-16) and (32) used for tuning the gains the resulting trajectory is more regular (red line in figure 7). Further investigations will focus on the definition of an adaptive gain tuning and on the inclusion of the ROV dynamic model in the simulator.

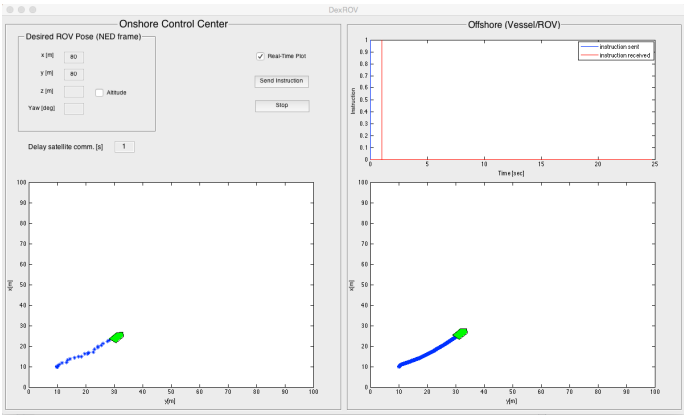

Fig. 3. Screenshot of the simulator.

6. CONCLUSIONS

In this paper the guidance (i.e. kinematics based) control design of the motion controller for an underwater remotely operated vehicle has been described. The proposed solution will be exploited within an European Commission H2020 research project called DexROV. The main contribution consists in having designed a kinematics guidance controller embedding in a common framework several different elementary motion control primitives. This solution is expected to significantly simplify the integration of the manipulator control system in the final architecture. The paper reports simulation results including sensor models, communication delays and unknown constant (in NED frame) ocean currents.

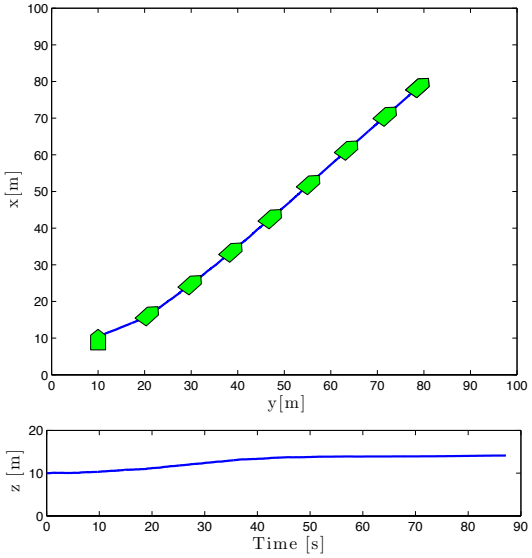

Fig. 4. Trajectory at low depth (10 m).

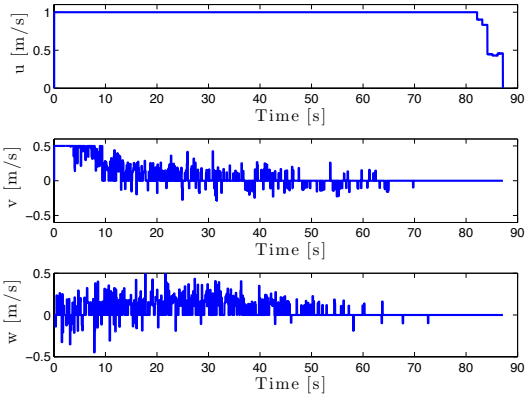

Fig. 5. Linear velocity commands at low depth (10 m).

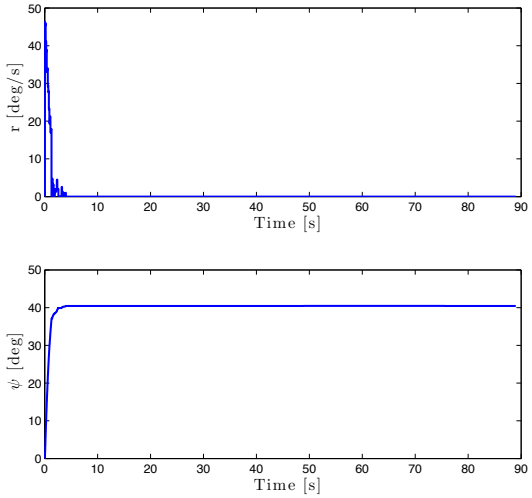

Fig. 6. Angular velocity commands and heading at low depth (10 m).

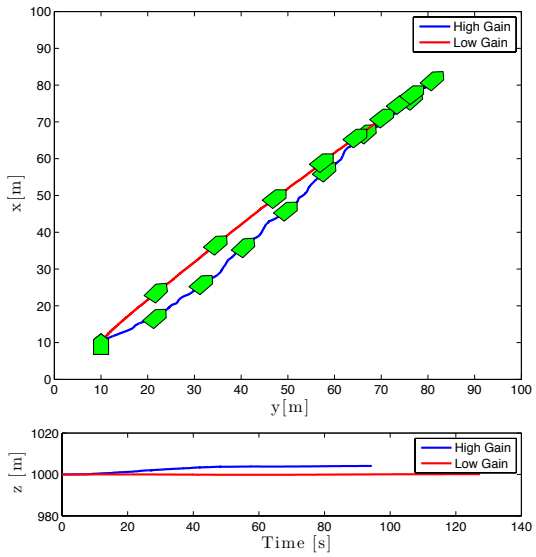

Fig. 7. Trajectory at high depth (1000 m).

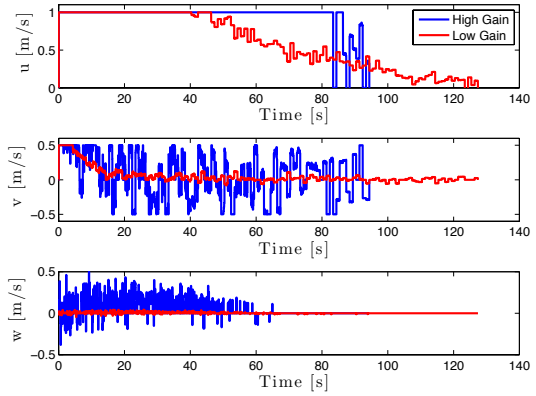

Fig. 8. Linear velocity commands at high depth (1000 m).

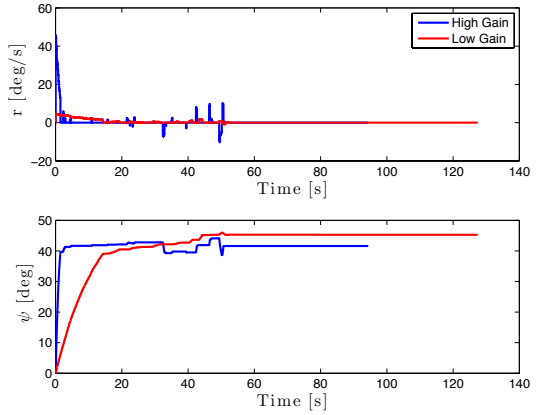

Fig. 9. Angular velocity commands and heading at high depth (1000 m).

REFERENCES

Christ, R.D. and Wernli, R.L. (2014). *The ROV Manual (Second Edition)*. Butterworth-Heinemann, Oxford, second edition.

Fossen, T.I. (2011). *Handbook of Marine Craft Hydrodynamics and Motion Control*. John Wiley & Sons, Ltd. doi:10.1002/9781119994138. URL http://dx.doi.org/10.1002/9781119994138.

Gancet, J., Urbina, D., Letier, P., Ilzokvitz, M., Weiss, P., Gauch, F., Antonelli, G., Indiveri, G., Casalino, G., Birk, A., Pfingsthorn, M.F., Calinon, S., Tanwani, A., Turetta, A., Walen, C., and Guilpain, L. (2015). DexROV: Dexterous undersea inspection and maintenance in presence of communication latencies. In *4th IFAC Workshop onNavigation, Guidance and Controlof Underwater Vehicles NGCUV 2015. Dedicated to the memory of Professor Geoff Roberts*, volume 48, 218 – 223. doi:10.1016/j.ifacol.2015.06.036. URL http://dx.doi.org/10.1016/j.ifacol.2015.06.036.

Hoang, N.Q. and Kreuzer, E. (2007). Adaptive PD-controller for positioning of a remotely operated vehicle close to an underwater structure: Theory and experiments. *Control Engineering Practice*, 15(4), 411 – 419. doi:10.1016/j.conengprac.2006.08.002. URL http://dx.doi.org/10.1016/j.conengprac.2006.08.002.

Sørensen, A.J., Dukan, F., Ludvigsen, M., de Almeida Fernandes, D., and Candeloro, M. (2012). Development of dynamic positioning and tracking system for the ROV Minerva. In *Further Advances in Unmanned Marine Vehicles*, Control, Robotics and Sensors Series, chapter Development of dynamic positioning and tracking system for the ROV Minerva, 113–128. Institution of Engineering and Technology. doi:10.1049/PBCE077E_ch6. URL http://dx.doi.org/10.1049/PBCE077E_ch6.

Sørensen, A.J. (2011). A survey of dynamic positioning control systems. *Annual Reviews in Control*, 35(1), 123 – 136. doi:10.1016/j.arcontrol.2011.03.008. URL http://dx.doi.org/10.1016/j.arcontrol.2011.03.008.

Sørensen, A.J. (2014). Dynamic positioning control systems for ships and underwater vehicles. In J. Baillieul and T. Samad (eds.), *Encyclopedia of Systems and Control*, 1–10. Springer London. doi:10.1007/978-1-4471-5102-9_122-1. URL http://dx.doi.org/10.1007/978-1-4471-5102-9_122-1.

Yoerger, D., Newman, J., and Slotine, J.J. (1986). Supervisory control system for the JASON ROV. *Oceanic Engineering, IEEE Journal of*, 11(3), 392–400. doi:10.1109/JOE.1986.1145191. URL http://dx.doi.org/10.1109/JOE.1986.1145191.